Atlas-based Segmentation using a Model of Lesion Growth

M. Bach Cuadra*, J. Gomez*, P. Hagmann*, C. Pollo**
J.-G. Villemure**, B.M. Dawant***, J.-P. Thiran*

*Signal Processing Institute (ITS), Swiss Federal Institute of Technology (EPFL)
CH-1015 Lausanne, Switzerland
Email: {Meritxell.Bach,JP.Thiran}@epfl.ch, http://ltswww.epfl.ch/~brain

**Department of Neurosurgery, Lausanne University Hospital (CHUV)
CH-1011 Lausanne, Switzerland
Email: Claudio.Pollo@chuv.hospvd.ch

***Department of Electrical and Computer Engineering
Vanderbilt University, Nashville, Tennessee
Email: Benoit.Dawant@vanderbilt.edu

ITS Technical Report 02.05

Abstract— **We propose a method for brain atlas deformation in presence of large space-occupying tumors or lesions, based on an *a priori* model of lesion growth that assumes radial expansion of the lesion from its central point. Atlas-based methods have been of limited use for segmenting brains that have been drastically altered by the presence of large space-occupying lesions. Our approach involves four steps. First, an affine registration brings the atlas and the patient into global correspondence. Secondly, a local registration warps the atlas onto the patient volume. Then, the seeding of a synthetic tumor into the brain atlas provides a template for the lesion. The last step is the deformation of the seeded atlas, combining a method derived from optical flow principles and a model of lesion growth. Results show that a good registration is performed and that method can be applied to automatic segmentation of structures and substructures in brains with gross deformation, with important medical applications in neurosurgery, radiosurgery and radiotherapy.**

I. Introduction

The use of deformable models to segment and project structures from a brain atlas onto a patient's MRI image is a widely used technique. Potential applications for the methods using deformable models include segmentation of structures and substructures of the patient's brain for radiation therapy and presurgical planning.

But, when large space-occupying tumors or lesions drastically alter shape and position of brain structures and substructures, atlas-based methods have been of limited use. The purpose of this work is to deform a brain atlas onto a patient's MR image in the presence of large space-occupying tumors or lesions. Our work is based on the pioneer works of Dawant, Hartmann and Gadamsetty [1]. In this method a brain atlas is first affinely registered to the patient's image. Then a non-linear deformation is performed in order to bring local correspondence between the atlas and the patient. After that, the brain atlas is "seeded" with a synthetic tumor or lesion centered on the centroid of the patient's tumor or lesion, and finally the "seeded" atlas is deformed to completely match the patient.

In our work, instead of relying on the deformation calculation of the non-linear registration algorithm on all the image, we apply an *a priori* model of tumor growth inside the tumor area, which assumes that the tumor has grown from its centroid in a radial fashion. As it will be shown, this model allows the placing of a smaller lesion "seed" (in comparison with [1]) into the brain atlas and, therefore, minimizes the amount of atlas information that is masked by the tumor "seed" voxels.

Moreover, the method proposed at [1] is also improved by performing an automated segmentation of the patient's lesion. The segmentation method used is the *Adaptive Template Moderated Spatially Varying Statistical Classification (ATM SVC)* algorithm proposed by Warfield et al.[2] [3]. This segmentation method performs a statistical classification (k-Nearest Neighbors rule) of the image voxels based on intensity and anatomical localization features. The results obtained with this segmentation method show that a wide range of lesions can be accurately segmented, including meningiomas, low grade gliomas, astrocytomas, multiple sclerosis and cardio-vascular accidents.

As for the validation, we present results obtained on real patient images together with the assessment by an expert. These results show that an atlas registration onto a patient with large space-occupying lesions is well performed even

when small lesion seed is placed into the brain atlas.

II. Data sets and method

A. Data sets

The patient images have been retrieved from the Surgical Planning Laboratory (SPL) of the Harvard Medical School & NSG Brain Tumor Database [1]. They consist in volumes of 128 coronal slices of 256 x 256 pixels and 0.9375 x 0.9375 x 1.5 mm^3 of voxel size. The digital atlas used in this work also comes from the SPL [4]. It is made of MR data from a single normal subject scanned with high resolution $256 \times 256 \times 160$ volume data set in coronal orientation with $0.9375 \times 0.9375 \times 1.5$ voxel size.

B. Seeded atlas deformation method

The approach we propose to solve the atlas-based segmentation problem when space occupying lesions are present is based on the *seeded atlas deformation* method (SAD) presented by Dawant et al. in [1]. As represented in Fig. 1 this method involves the following steps:

- A transformation of nine degrees of freedom is computed to globally register the atlas and the patient volume.
- A first non-rigid registration is applied. This performs a first atlas deformation to warp the image patient and, since the atlas doesn't have any tumor, nothing happens in the lesion area.
- The tumor is segmented manually outlining the lesion in the patient image.
- Highlighting of the intensity inside the tumor contour is then performed using an intensity level different from the surrounding tissues.
- Erosion is applied to the tumor mask (using morphological operations) to create the seed mask.
- This seed is placed in the first non-rigidly deformed atlas.
- A second non-rigid registration is then applied allowing this time a more elastic deformation.

The *demons* algorithm of J.-Ph. Thirion is used for the non-rigid registration [5]. For each voxel a displacement vector is found. The regularity of the displacement field is imposed by a Gaussian filtering to regularize the free form deformation. The standard deviation (σ parameter) of the filter is used to change the characteristics of the matching transformation. See section II-C.2 for details. The SAD method leads to good results (as it could be seen in section III), but it also presents some weak points. Specifically there is an important compromise to be found between the seed size and the elasticity of the model, governed by σ. To obtain a realistic deformation of the brain a large σ has to be chosen but that means not too much deformability of the model. In this case, a relatively big seed must be introduced to obtain a good seed deformation. Therefore a large region of original atlas information is lost because it is masked. Finally, seed deformation is also strongly dependent of the number of iterations of the algorithm (more iterations are needed since large morphological differences still exist). In the next section we detail the method we propose, modifying the work of [1] to improve the robustness of the seeded atlas deformation method.

[1] http://spl.bwh.harvard.edu:8000/~warfield/tumorbase

Fig. 1. Scheme of seeded atlas deformation method.

C. Model of Tumor Growth

Our approach introduces two main differences with respect to the SAD method. First, automated segmentation of the patient's lesion is performed instead of manually drawing the tumor contour. Second, we apply an a priori model of tumor growth inside the lesion area, which assumes that the tumor has grown from its centroid in a radial way. This last improvement introduces significant advantages to the initial approach. The most important one is that there is no more dependency to the seed size, neither to the elasticity parameter of regularization, nor to the number of iterations. Our Model of Tumor Growth (MTG) is developed with the following steps:

- An affine transformation is applied to the brain atlas in order to globally match the patient's volume.
- After the global transformation, a non-linear registration is performed with the objective of bringing the atlas and the patient volumes in local correspondence. The lesion is then automatically segmented but is no more necessary to highlight it.
- After that, the warped atlas is seeded with a small synthetic lesion placed at the centroid of the patient's lesion.
- Finally, the non-linear registration algorithm is performed again in order to deform the seeded atlas to match the patient. In this step, the non-linear registration algorithm is not applied to the whole volume, but only to the area outside the tumor location. In the tumor location area, an *a priori* model of tumor growth is used, which assumes that the tumor started growing at its centroid and expanded in a radial way.

The result after applying these steps is a deformed brain atlas in which a tumor has grown from an initial seed, causing displacement and deformation to the surrounding tissues. After this, structures and substructures from the brain atlas may be projected to the patient's image.

C.1 Affine transformation

Before performing the non-rigid deformation algorithm, it is necessary to bring the atlas and patient volumes into global correspondence. This step is compulsory because the *demons* algorithm needs overlapping of the patient and atlas structures in order to being able to match them. This global correspondence is brought by applying an affine

transformation to the brain atlas. The chosen affine transformation is the one proposed by Cuisenaire, Thiran, Macq, Michel, De Volder and Marques [6]. The global transformation $\boldsymbol{y} = T(x)$ from the patient cortical surface to the atlas cortical surface is modeled by a linear combination of N elementary scalar functions $f_j(x)$ for each coordinate $y_i (i = 0, 1, 2)$ of $\boldsymbol{y}$. Formally,

$$y_i = \sum_{j=0}^{N-1} \alpha_{ij} \cdot f_j(x). \quad (1)$$

A general 3D first degree transform is represented with $N = 4$ and $f_j(x) = 1, x_0, x_1, x_2$, and thus 12 coefficients α_{ij}. Finally, the global transformation looks for the coefficients that minimize the Euclidian distance between the atlas cortical surface to the correspondent cortical surface in the target image. For more details refer to [6].

C.2 Non-rigid deformation algorithm

After the global transformation, a first non-linear registration is performed with the objective of bringing the atlas and the patient volumes in local correspondence. Relying on our previous experience, we also use here the *demons* algorithm proposed by J.-Ph. Thirion [7] [5] [8]. This method approaches the problem of image matching as a diffusion process, in which object boundaries in one image (reference image) are viewed as semi-permeable membranes. The other image (floating image) is considered as a deformable grid, and diffuses through these interfaces driven by the action of effectors (also called *demons* by analogy with Maxwell's demons) situated within the membranes. Various kinds of *demons* can be designed to apply this paradigm to specific applications. In the particular case of voxel-by-voxel intensity similarity, the *demons* paradigm is similar to optical flow methods. The implementation of the computation of the displacement vector for each voxel that has been used in this study is the one shown below.

$$\overrightarrow{v}_{I_2 \to I_1} = \frac{(I_2 - I_1)\overrightarrow{\nabla} I_1}{\overrightarrow{\nabla} I_1^2 + (I_2 - I_1)^2}, \quad (2)$$

where I_1 and I_2 are the intensity values of the images to be matched. In this approach, global smoothness of the displacement field is not enforced. Rather than using a global regularization method, a more local constraint imposing similar displacements for nearby voxels can be imposed by smoothing this field with a Gaussian filter. This key issue of the demons algorithm is treated in detail in section VI.

Large morphological differences between image volumes could render optical flow methods completely ineffective because the assumption of small displacement is violated. In order to make the algorithm more robust to large differences, the deformation algorithm is applied in a hierarchical way. Also, a mechanism has been implemented that maintains consistency between the forward and the reverse deformation fields. As proposed in [5] this is done by computing the deformation field T_{12} (the deformation field warping image 1 onto image 2) and the deformation field T_{21} (the deformation field warping image 2 onto image 1) and distributing the residual $R = T_{12} \circ T_{21}$ onto these two fields. This bijective implementation, coupled with the smoothing of the field, preserves the image anatomy. It also provides a way to obtain the inverse transformation.

C.3 Lesion segmentation

In order to apply the deformation method, a segmentation of the patient's lesion is needed. This segmentation will be used first for the generation of the synthetic lesion seed and, second, for the construction of the model of tumor growth. The automated segmentation algorithm that has been used in this study is the *Adaptive Template Moderated Spatially Varying Statistical Classification (ATM SVC)* algorithm proposed by Warfield, Kaus, Jolesz and Kikinis [2] [3]. The *ATM SVC* algorithm overcomes the limitations of spectral segmentation techniques and deformable models segmentation techniques by embedding a traditional k-Nearest Neighbors (k-NN) classification into a higher dimensionality problem space. The additional dimensionality is derived from a brain atlas, and acts to moderate the statistical classification. The *ATM SVC* algorithm consists on three steps that are performed iteratively. The first step is a k-NN classification that classifies the image voxels into each one of the classes. The second step is a non-rigid matching between the segmented image and a brain atlas labeled with the same classes. Finally, spatial localization features are extracted from the brain atlas. This features will act as maps of certainty of anatomical localization.

Previous to the segmentation, a manual prototype selection must be performed for each class. This prototype selection process will store the spatial location of the prototypes and, therefore, it will make possible the calculation of any of the desired classification features. The number of prototypes per class that has been used in this work is between 50 and 100. For this number of prototypes, it can be proved that a value of the k parameter of the k-NN classification between 5 and 7 is optimal (see [9] for details). The classes that are used for the lesion segmentation in this study are: *ventricles*, *lesion* and *"rest of the brain"*.

The *ATM SVC* algorithm consists on three steps that are performed iteratively. The first step is a k-NN classification that classifies the image voxels into each one of the classes. The second step is a non-rigid matching between the segmented image and a brain atlas labeled with the same classes. Finally, spatial localization features are extracted from the brain atlas. This features will act as maps of certainty of anatomical localization so that, when the existing feature channels have insufficient contrast to identify a structure, the anatomical localization can provide weighting for the prototypes from which the classification for a voxel is computed. As the anatomical localization weighting increases, the contrast in feature space between the different structures increases.

The spatial localization features are extracted from the brain atlas progressively: first a *distance to the edges of the brain* feature, then a *distance to the atlas ventricles*

(a) (b) (c)

Fig. 2. Segmentation results obtained with the *ATM SVC* algorithm on various lesion and tumor types. Red: manual segmentation. Green: *ATM SVC* segmentation. (a) Meningioma with left parasellar location. (b) Low grade glioma with right frontal location. (c) Cardio-vascular accident.

feature. This is done in order to ensure that they really model anatomical localization in the patient image (i.e., they are extracted from the atlas structures that have already been matched).

A good matching between the segmented image and the labelled atlas is ensured by inserting the classes and the features progressively. This means that the first classification step will classify all the patient's voxels as belonging to the *"rest of the brain"* class and, after this, the brain surfaces of the atlas and patient will be matched, and the *distance to the edges of the brain* feature will be extracted. The second classification step will use as classification features image intensity and *distance to the edges of the brain*; the classes in which the patient's voxels will be classified are *ventricles* and *"rest of the brain"*. After this, a non-rigid deformation will be performed on the brain atlas in order to bring correspondence between the patient and atlas ventricles. Then, the *distance to the atlas ventricles* feature is calculated. Next, a classification step is performed which will classify the patient's voxels using all the classes and all the spatial localization features extracted from the atlas, as well as image intensity. At this point, a first segmentation of the lesion is obtained, and a *distance to the lesion* feature is computed by using this first lesion segmentation (treated with morphological operations). Finally, the last classification step using all the features gives as result the final segmentation of the patient's lesion. Sample results for various lesion types are displayed in Fig.2. This results have been obtained by applying the *ATM SVC* algorithm with $k = 7$ for the k-NN classification, and using 100 prototypes for each one of the classes. The deformation algorithm used to register the segmented images with the labeled atlas is the *demons* algorithm, that is the subject of the next subsection. In the figure, the accuracy of the *ATM SVC* segmentation is assessed by comparing it with manual segmentations performed by experts.

C.4 Atlas seeding

After the first two steps of the proposed algorithm (i.e. affine transformation and a first atlas deformation using demons algorithm), the atlas and the patient volumes are in correspondence except in regions that have been drastically deformed by the tumor. By eroding the lesion segmentation mask obtained with the *ATM SVC* algorithm, the mask of the lesion seed is generated. At the points marked by the seed mask, atlas voxels are replaced by patient tumor voxels. This way, a synthetic tumor seed has been inserted into the atlas volume. It should be noted that the size of the seed , in terms of loss of atlas information, should be as small as possible.

C.5 Non-rigid deformation using a model of tumor growth

At this point, there is a template of lesion in the brain atlas, and there is an overlap between it and the patient's lesion. The *demons algorithm* is applied outside the lesion area. Inside the tumor region a model of tumor growth is applied. This model consists in assuming a radial growth of the tumor from the tumor seed contour. The model of tumor growth is implemented in two steps. First, the distance map is calculated to measure the distance from the seed border to the tumor border.

As we have seen in section II-B Dawant et al.[1] use the *demons* algorithm with a low value of the Gaussian filter's standard deviation ($\sigma = 0.5$) in order to deform very elastically the atlas to match the patient. They also highlighted the patient's lesion and the atlas seed, so that they were assigned an intensity value different from the surrounding tissues. This was done in order to mark the *inside-outside* polarity of the *demons* deformation, and also to force the *demons* algorithm to place *demons* (i.e., effectors) at the boundaries of the lesion and lesion seed. But as we have said before, too much elasticity in the algorithm can lead in a non realistic deformation of the brain from an anatomical point of view. In our MTG method, since we do not use the *demons* algorithm inside the tumor region, we do not need to highlight the lesion and lesion seed neither use a so elastic sigma parameter. In our work, the elastic *demons* deformation is used with $\sigma = 1$. We had previously found that this sigma value lead in very good results for atlas-based segmentation of normal anatomy (see Appendix and [10]).

Inside the tumor region that has been delimited by the *ATM SVC* segmentation, a model of tumor growth is applied instead of the *demons* algorithm. This model consists on assuming a *radial* growth of the tumor from the borders of the tumor seed. By using this model, dependence on the number of iterations of the non-rigid deformation algorithm is eliminated. Moreover, convergence to the target (i.e., the

(a) (b)

(c)

(d)

Fig. 3. (a) Direction of the deformation field inside lesion area, it corresponds to the gradient of the distance seed map. The central structure that can be distinguished as the whitest part corresponds to the big seed. (b) Deformed atlas. (c) Total deformation combining demons algorithm deformation outside the tumor and the model of lesion growth deformation inside the lesion area, it corresponds to image (b). (d) Zoom of figure (c) at lesion area.

Fig. 4. Adaptive calculation of the deformation force applied inside the lesion area (model of tumor growth).

lesion seed) is ensured, while if relying on the non-rigid deformation algorithm, as in [1], it is not possible to ensure that the tumor seed will spread in all the atlas voxels in the lesion region, since there is a dependence on the intensity gradient at this region.

The model of tumor growth is implemented in two steps. The first step is the calculation of a distance map that measures the distance from the seed border to the border of the tumor. This is done using the method proposed by Saito and Toriwaki[11]. This distance map, therefore, indicates how far the voxels are inside the tumor region with respect to the seed. This values will be used as the module of the deformation vector for each voxel inside the tumor area. The second step is the calculation of the gradient of this distance map. This gradient will indicate the direction of the shortest path leading to the lesion seed, and it will be used as the direction of the deformation force for each voxel inside the tumor area. Note that radial term is not used here in terms of a direction normal to the contour but as the shortest path (see Fig. 3(a)).

Therefore, the formal expression of the displacement vector inside the lesion area is the one shown below.

$$\overrightarrow{v}_{lesion} = -\frac{D_{seed} \cdot \overrightarrow{\nabla} D_{seed}}{N_{iterations}}, \qquad (3)$$

where D_{seed} is the distance map computed from the seed border to the outside of the seed, and $N_{iterations}$ is the number of iterations of the deformation algorithm that have to be performed. So, a displacement vector is computed at every voxel using either the demons algorithm or the tumor growth algorithm. Then, the entire field is regularized with $\sigma = 1$ to avoid possible discontinuities (see Fig. 3(b)). By proceeding in this way, the growth of the seed is tracked and the deformation force is adapted to the variations of this growth. This adaptive process is illustrated in Fig. 4. By using the model of lesion growth, dependence on the number of iterations of the non-rigid deformation algorithm is eliminated (see Eq. 3).

III. Results and Validation

A. Deformed atlas images

The algorithm has been tested and validated on 6 different patients having either meningioma or low grade glioma, all leading in similar results. The initial images (patient and seeded atlas) and the resulting deformed atlas for a patient with left parasellar meningioma are shown in 5. The performance of our method (MTG) and the *seeded atlas deformation* (SAD) method are compared for different sizes of the tumor seed that is inserted into the brain atlas. Segmentation results (see Fig. 5(a)) have been obtained by applying the *ATM SVC* algorithm with $k = 7$ for the k-NN classification, and using 100 prototypes for each one of the classes. Two lesion contours are shown[t2]: the red one corresponds to an expert manual segmentation and green one to the ATM SVC segmentation. Patient's tumor size is 41.25 x 42.1875 x 52.5 mm^3. Two seed sizes have been used for our experiments: the biggest one has size 16.875 x 16.875 x 24.0 mm^3 and the smallest has size 10.3125 x 10.3125 x 12.0 mm^3 (Fig. 5(b)) and Fig. 5(c)). As the results show, the SAD method achieves results that are comparable to those of our method, when using the big seed (note that deformation vector filed is almost the same for both methods). But when using the small one, for the SAD method, the deformation inside the tumor area does not reach the target while the method using the model of tumor growth (MTG) does. In the SAD method, the force on the lesion contour is actually misguided. It should also be noted that the MTG method performs in a very similar way for both seed sizes (compare Fig. 5(i) and Fig. 5(k)). This different behavior can be explained as follows. While the SAD method relies on the intensity gradient for the deformation inside the tumor area, the MTG method uses a model that applies the deformation independently from the intensity gradient and using only *a priori* information (i.e. a model of tumor growth). In the first case, there is a strong gradient on the tumor and seed contour due to the highlighting. But between them, just the atlas gradient is used to lead the direction of the deformation inside tumor area. This gradient information is not enough when using a small seed since a large deformation is need. That explains the dependency of SAD method on the seed size and iteration number. On the contrary, MTG can compensate these large differences thanks to the growing model. However, there exists a minimum number of pixels that have to be defined for the small seed if we want to guarantee the vector field to converge inside the lesion area.

B. Segmentation results study

In this section, structures and substructures from the deformed brain atlas have been projected to the patient's image. The model of lesion growth leads to a good starting point for segmentation of deep structures in the brain. A perfect seed deformation onto the lesion has been obtain. The structures that were initially inside the region area have been completely pushed out of the lesion contour even if they have not perfectly reached their target (see Fig. 6). However, a little imprecision could exist due to the regularization step. The use of a regularization parameter such as $\sigma = 1.0$ can cause some misguiding in the lesion contour because of the interaction between deformation field inside and outside lesion area. So we have to consider that we have a significant contribution of the radial force outside and in the lesion contour since we are filtering the total

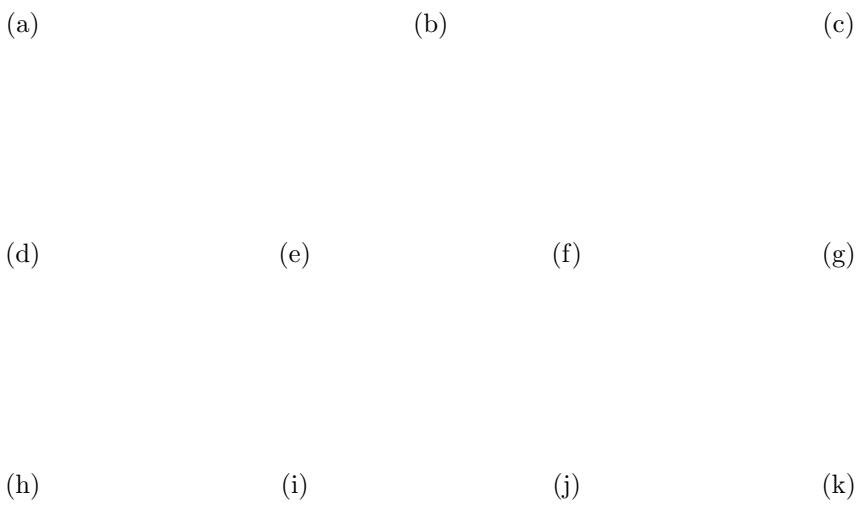

Fig. 5. Atlas seeding, lesion growth and deformation field analysis. (a) Patient with left parasellar meningioma. (b) Warped atlas, big seed. (c) Warped atlas, small seed. (d) Deformation of seeded atlas with the big seed using SAD. (e) Deformation of seeded atlas with the big seed using MTG. (f) Deformation of seeded atlas with the small seed using SAD. (g) Deformation of seeded atlas with the small seed using MTG. (h) SAD: deformation module using a big seed. (i) MTG: deformation module using a big seed. (j) SAD: deformation module using a small seed. (k) MTG: deformation module using a small seed.

Fig. 6. Segmentation analysis: model of lesion growth method applied to small seed. Lesion, ventricles and central nuclei system are segmented. (a) Axial view. (b) Sagital view.

deformation field. It might be possible that the lesion area pulls in some way the rest of the structures to the seed position. Another important point to consider is how sensible the final result is with respect to the initial seed position. This study is performed in next subsection.

C. Seed position variability

We have no *a priori* knowledge about lesion size or position. Actually, for some kinds of lesions such as the glioma a central seed growing equally in all directions is a realistic model. However, for other tumors, like a meningioma, it would be more realistic from a biomedical point of view to consider a seed placed at the external border of the tumor since this kind of lesions starts at the dura mater (in brain surface). We present hereafter the segmentation results obtained from different seed positions. Lesion, ventricles and central nuclei system have been studied. Variation have been performed with seed translations from 4mm to 9mm in the three main directions. We have obtained the same segmentation results in almost all cases. Quantitative measures such as the maximum displacement, the mean and variance of the vector field norm are shown in table I. It can be seen that for all displacements the mean transformation field remains the same. Just a region of interest of 3cm around the tumor has been considered. Segmentation results have been also validated visually by an expert (C.P.).

IV. Discussion and Future work

To the best of our knowledge, the work presented here is not the first attempt at atlas-based segmentation when large occupying tumors exists. We are of course thinking about [1] and also [12]. The main difference between [1] or us and [12] is that ours methods aren't based on biomechanical models. In [12] is also necessary not only a gray mater, white mater, and cerebrospinal fluid segmentation but also

Displacement	center	+4X	-4X	-6X	+4Y
Max	19.18	16.83	21.62	22.83	20.59
Mean	4.17	3.75	3.80	3.96	3.79
Variance	8.16	9.41	10.7	12.58	9.98
Displacement	-4Y	+6Y	+6Z	-6Z	-9Z
Max	19.56	22.61	18.05	23.32	19.63
Mean	3.76	3.93	3.71	4.01	3.89
Variance	10.67	11.65	9.53	13.44	11.89

TABLE I

VARIABILITY STUDY WITH SMALL SEED. ALL VALUES ARE IN MILLIMETERS AND PER VOXEL. MAXIMUM VALUE, MEAN AND VARIANCE OF THE VECTOR FIELD NORM ARE SHOWN.

a very accurate a priori knowledge about ventricules size of patient image. We are completly agree with Dawant et al. in the idea that lack of an explicit underlying mathematical model in the seeded atlas deformation method is both its strength and its potential weakness. The *seed atlas deformation algorithm* is simpler and faster than [12]. But this simplycity (the consistency of the deformation field relies only in the regularization parameter) is at the same moment the weak point since the size of the smoothing filter becomes a critical choice to get or not good results. The method we propose try to increase the robustnes of the seeded atlas deformation method leading their method independent to the seed size and to the number of iterations and, the most important, doing [1] much less sensitive to the regularization parameter. Of course the use a such a simple model of tumor growth can be questionable. Even if no study clearly discuss this, it is reasonable to believe that some lesions grow radially if they have no constraint (bone, dura circumvolution, etc.) Meningioma, low grade glioma, but also metastasis or abscesses, can follow this model.

However, new aspects have to be considered now. We think about introducing an adaptative filtering depending on the distance to the tumor. This different smoothing could prevent too much influence of the radial motion of the lesion area. We could distinguish three main different areas that would be smoothed differently: the healty brain, the area limiting the lesion and the lesion area. The healthy brain would had been smoothed with the experimental parameter found for the atlas-based segmentation in healty anatomy ($\sigma = 1.0$). Then, the area limiting the lesion would be filtered less elastically and, finally, no smoothing at all would be performed inside the lesion area. This could be the solution for the misguided force in the limit of the lesion due to inlfuence of the deformation field outside the tumor area. We could imagine also that using this adaptative filtering wouldn't be necessary any more to apply twice the *demons* algorithm (once with $\sigma = 2.0$ and once with $\sigma = 1.$) but only once using the adaptative filtering.

Another point to study could be to consider the same algorithm in two steps. In our opinion, this will probably lead to a best final segmentation. First, only perform the lesion growth. Second, perform the non-rigid registration between the atlas (where lesion has already pushed out all structures outside tumor area) and the patient image. This way we apply the non-rigid registration with almost the best positioning for the structures affected by the lesion.

Also, the variability of the seed position will be studied in more detail in a future work. A first study has been presented in section III-C. Since there isn't any *a priori* knowledge about the lesion growing in the brain so there is no aparent reason to say that the lesion is growing up from its center. However, he have seen that placing the seed at many different positions don't represent such much different segmentation results.

Finally, in a more evolved method it would be also very important to consider some anatomical constraints of the structures of interest introducing for example some shape analysis of the most important structures near the lesion.

V. Conclusion

We proposed a new approach for brain atlas deformation in the presence of large space-occupying tumors, which makes use of a simple model of tumor growth. The use of an *a priori* model for the brain atlas deformation inside the tumor area enables a good matching, even when brain structures have been drastically altered by the presence of a tumor. Results show that our method overcomes the limitation such as the "seed" size dependence and convergence to the target that the most similar article in the literature had. Finally, the model of lesion growth method improves the robustness of the seeded atlas deformation method since it is not so sensitive to the choice of the regularization parameter.

VI. Acknowledgement

This work is supported by the Swiss National Science Foundation grants numbers 21-55580-98 and 20-64947.01.

Appendix

The *demons algorithm* [5] is used here for the non-rigid registration in either the ATMSV method and in the atlas-based segmentation. As we have seen in section II-B and in section II-C.2, one of the key aspects of *demons algorithm* [5] is its simple regularization technique to compensate the ill-posed problem coming frome the optical flow principle. Cahier et al.[8] have demonstrated that, in this case, this regularization could be implemented as the smoothing of the displacement field by a Gaussian kernel. So, the elasticity of the deformation depends only on the standard deviation of the Gaussian filter. The larger the standard deviation of the filter, the less elastic the transformation. That is completly logical since a larger sigma represents a larger neighborhood influence. We have run the algorithm for different sigma values in order to study the influence of it in either the resulting deformed images and deformation field. Both a distance metric between images and the roughness of the transformation field are considered and the study is limited to healthy brain images (see the atlas model and the target in Fig. 7).

(a) (b)

Fig. 7. (a) Target image. (b) Deformable model.

(a) (b) (c) (d) (e)

Fig. 8. (a) Deformed images using demons algorithm. (a) Sigma 0.5. (b) Sigma 1.0. (c) Sigma 1.5. (d) Sigma 2.0. (e) Sigma 2.5.

We have first run the algorithm for sigma 0.5,1,1.5,2 and 2.5 (that represents 3,5,7,9,11 Gaussian coeffcients respectivetly) to see the effect of different elasticities. Logically, since sigma is increasing the algorithm performs less elastically and too large differeces can not be matched. Results presented in Fig. 8 shown that the largest deformations cannot be achieved for sigma values bigger than 1.5. The sum of squared differences (SSD) has been calculated between deformed atlas and target image intensities to quantify the matching quality of the algorithm. However, validation of the algorithm in terms of smoothnes of the displacement field is an equally important issue in the case of non-rigid registration. Calculations has been done in both the whole image (without considering background) and in a small region of interest (ROI) containing the central nuclei, the ventricles and the thalamus. As we can see in Table II, in terms of SSD, the error is directly proportional to sigma value. The norm of the deformation field have been also analyzed to measure the roughness of the transformation: maximum displacement, mean displacement and variance of the deformation field have been calculated. Note that the statistics calculated in a ROI and in the whole image are almost the same in the case of maximum displacement and variance of the deformation field, that means, this ROI could represent the statistics in whole image. That is because this ROI contains the ventricles and they usually present the largest differences between images. Figure 9 shows the variance of the norm of deformation field calculated in the whole image versus sigma for different values between 0.4 and 1.2 (3 and 5 coefficients). Obviously, variance of the deformation field is decreasing while sigma is increasing. We would like to note that the demons algorithm is implemented in a multiscale way and that the same number of coefficients represent different filtered distances in every scale: in first scales we have a less elastic filtering (biggest morphological differences are compensated) and in latest scales much more elasticity is allowed. In our case we have chose sigma 1 since largest differences have been achieved and a less roughness deformation is performed. However, it is still difficult to define a critera to chose the *best* sigma parameter since there is not yet a gold standard for non-rigid registration validation.

Fig. 9. Variance of deformation field calculated in whole image for different sigma from 0.4 until 1.2.

References

[1] B. M. Dawant, S. L. Hartmann, and S. Gadamsetty, "Brain Atlas Deformation in the Presence of Large Space-occupying Tumors," in *MICCAI*, pp. 589–596, 1999.

[2] S. K. Warfield, M. Kaus, F. A. Jolesz, and R. Kikinis, "Adaptive, Template Moderated, Spatially Varying Statistical Classification," *Medical Image Analysis*, vol. 4, pp. 43–55, March 2000.
[3] M. Kaus, S. Warfield, A. Nabavi, E. Chatzidakis, P. Black, F. Jolesz, and R. Kikinis, "Segmentation of Meningiomas and Low Grade Gliomas in MRI," in *MICCAI*, pp. 1–10, 1999.
[4] R. Kikinis and et al., "A digital brain atlas for surgical planning, model driven segmentation and teaching," *IEEE Transactions on Visualization and Computer Graphics*, vol. 2, no. 3, 1996. http://splweb.bwh.harvard.edu:8000.
[5] J.-P. Thirion, "Image matching as a diffusion process: an analogy with Maxwell's demons," *Medical Image Analysis*, vol. 2, no. 3, pp. 243–260, 1998.
[6] O. Cuisenaire, J.-P. Thiran, B. Macq, C. Michel, A. D. Volder, and F. Marques, "Automatic Registration of 3D MR images with a Computerized Brain Atlas," in *SPIE Medical Imaging*, vol. 1719, pp. 438–449, 1996.
[7] J.-P. Thirion, "Fast Non-Rigid Matching of 3D Medical Images," Tech. Rep. 2547, INRIA, May 1995.
[8] P. Cachier, X. Pennec, and N. Ayache, "Fast Non-Rigid Matching by Gradient Descent: Study and Improvements of the "Demons" Algorithm," Tech. Rep. 3706, INRIA, June 1999.
[9] E. Solanas, V. Duay, O. Cuisenaire, and J.-P. Thiran, "Relative anatomical location for statistical non-parametric brain tissue classification in MRI images," in *ICIP*, October 2001.
[10] M. Bach, O. Cuisenaire, R. Meuli, and J.-P. Thiran, "Automatic segmentation of internal structures of the brain in MRI using a tandem of affine and non-rigid registration of an anatomical atlas," in *ICIP*, October 2001.
[11] T. Saito and J. Toriwaki, "New algorithms for euclidean distance transformation of an n-dimensional digitised picture with applications," in *Pattern Recognition*, vol. 27, pp. 1551–1565, 1994.
[12] S. Kyriacou and C. Davatzikos, "Nonlinear elastic registration of brain images with tumor pathology using a biomechanical model," *IEEE Trans. Med. Imaging*, vol. 18, no. 7, pp. 580–592, 1999.

		Whole Image				ROI			
Sigma	Coefficients	SSD	Max	Mean	Variance	SSD	Max	Mean	Variance
0.5	3	22.11	11.7	0.8	1.6	0.37	9.41	3.46	2.2
1.0	5	37.03	7.3	0.7	0.7	0.76	6.95	2.7	1.03
1.5	7	47.7	5.5	0.67	0.38	1.38	4.99	2.27	0.56
2.0	9	52.6	4.06	0.61	0.23	1.9	3.67	1.89	0.32
2.5	11	56.5	2.99	0.56	0.15	2.37	2.85	1.6	0.2

TABLE II

Sum of Squared Differences error for different value of sigma in both the whole image and a ROI. Deformation field analysis: maximum displacement, mean and variance of the norm of the deformation field.